calculated estimates because of nonideal packing interactions or incomplete filling of the cavity.

Hydrophobicity, packing effects, cavity formation, and side chain conformational entropy all play important roles in determining protein stability and must be considered in any mutational study. Additional mutations coupled with intensive free energy calculations should provide greater insight into the various contributions of these factors to protein folding and stability. This approach can be applied to other forces that determine protein folding, including hydrogen bonding, electrostatic interactions, and main chain effects.

REFERENCES AND NOTES

1. K. A. Dill, *Biochemistry* **29**, 7133 (1990).
2. M. J. Behe, E. E. Lattman, G. D. Rose, *Proc. Natl. Acad. Sci. U.S.A.* **88**, 4195 (1991).
3. A. E. Eriksson *et al.*, *Science* **255**, 178 (1992).
4. M. Matsumura, W. J. Becktel, B. W. Matthews, *Nature* **334**, 406 (1988).
5. J. T. Kellis, Jr., K. Nyberg, D. Sali, A. R. Fersht, *ibid.* **333**, 784 (1988).
6. W. S. Sandberg and T. C. Terwilliger, *Science* **245**, 54 (1989).
7. K. Yutani, K. Ogasahara, T. Tsujita, Y. Sugino, *Proc. Natl. Acad. Sci. U.S.A.* **84**, 4441 (1987).
8. D. Shortle, W. E. Stites, A. K. Meeker, *Biochemistry* **29**, 8033 (1990).
9. W. A. Lim and R. T. Sauer, *J. Mol. Biol.* **219**, 359 (1991).
10. _____, *Nature* **339**, 31 (1989).
11. M. Karpusas, W. A. Baase, M. Matsumura, B. W. Matthews, *Proc. Natl. Acad. Sci. U.S.A.* **86**, 8237 (1989).
12. C. J. Noren, S. J. Anthony-Cahill, M. C. Griffith, P. G. Schultz, *Science* **244**, 182 (1989).
13. J. A. Ellman, D. Mendel, C. J. Noren, S. Anthony-Cahill, P. G. Schultz, *Methods Enzymol.* **202**, 301 (1991).
14. T. L. Doering *et al.*, *Science* **252**, 1851 (1991).
15. R. O. Heuckroth, L. Glaser, J. I. Gordon, *Proc. Natl. Acad. Sci. U.S.A.* **85**, 8795 (1988).
16. Phe adopted a low-energy dihedral angle (χ_1 = −56°) in a minimized isolated helix (Trp^{129} to Ala^{134}), suggesting that the unfavorable angle in the native protein is caused by unfavorable steric interactions with another residue within the core of the protein. That residue is Ser^{117}, which forms a hydrogen bond with the carbonyl O of the Asn^{132} side chain and is thus unlikely to move to accommodate Phe^{133}.
17. Mutagenesis was performed according to the Eckstein method with 5′ TCT ACT TTT AGC CTA GTT AAC TGC 5′ (mismatches underlined) as the mutagenic oligonucleotide; J. R. Sayers, W. Schmidt, F. Eckstein, *Nucleic Acids Res.* **16**, 791 (1988).
18. C. J. Noren *et al.*, *ibid.* **18**, 83 (1990).
19. D. Mendel, J. A. Ellman, P. G. Schultz, *J. Am. Chem. Soc.* **113**, 2758 (1991).
20. J. A. Ellman, D. Mendel, P. G. Schultz, *Science* **255**, 197 (1992).
21. Plasmid pHSe54,97.TA encodes a cysteine-free T4L behind a twin *tac* promoter.
22. Proteins were purified by polyethyleneimine·HCl precipitation of the crude in vitro suppression reaction followed by passing the supernatant over DEAE- and CM-cellulose cartridges in tandem. T4L's were eluted from the CM-cellulose cartridge with a salt gradient (pH 7.5). A second round of cation exchange chromatography at pH 4.9 afforded homogeneous protein. See also (*20*).
23. Suppression efficiencies, determined by scintillation counting of SDS-polyacrylamide gel slices, were used to estimate the amount of T4L produced. These values were then compared to the rates of lysis of *E. coli* strain NAPIV cells by the mutant proteins to estimate the specific activity relative to wild-type enzyme. See also (*19*) and (*20*).
24. P. C. Lyu, J. C. Sherman, A. Chen, N. R. Kallenbach, *Proc. Natl. Acad. Sci. U.S.A.* **88**, 5317 (1991).
25. W. J. Becktel and W. A. Baase, *Biopolymers* **26**, 619 (1987).
26. K. A. Sharp, A. Nicholls, R. Friedman, B. Honig, *Biochemistry* **30**, 9686 (1991); K. A. Sharp, A. Nicholls, R. F. Fine, B. Honig, *Science* **252**, 106 (1991).
27. A. Nicholls, K. A. Sharp, B. Honig, *Proteins* **11**, 281 (1991).
28. C. Chothia, *J. Mol. Biol.* **105**, 1 (1976).
29. Cavity terms can also be estimated from cavity surface areas (*3*). Changes in cavity surface areas using a 1.4 Å² probe are: Leu^{133} → **1**, −7.7 Å²; Leu^{133} → **2**, −14.6 Å²; Leu^{133} → **4**, 16.4 Å²; Leu^{133} → **6**, 66.1 Å². Estimates using these values give cavity terms similar to those reported in Table 2.
30. The only isosteric replacement provided by the natural amino acids is Val to Thr; however, this would result in the introduction of an unsatisfied hydrogen bond.
31. Octanol-water partition values were determined according to the protocol of J. Fauchere and V. Pliska [*Eur. J. Med. Chem.* **18**, 369 (1983)] by vapor phase chromatography. The $\Delta\Delta G$ value of 1.8 kcal mol^{-1} for **4** versus **5** represents the average of five determinations.
32. C. Schafmeister, LEaP, University of California, San Francisco (1991).
33. C. Huang *et al.*, MIDAS PLUS, Computer Graphics Lab, University of California, San Francisco (1991).
34. D. A. Evans, T. C. Britton, J. A. Ellman, R. L. Dorow, *J. Am. Chem. Soc.* **112**, 4011 (1990).
35. R. Naef and D. Seebach, *Helv. Chim. Acta.* **68**, 135 (1985).
36. G. Seibel, H. C. Singh, P. K. Weiner, J. Caldwell, P. A. Kollman, AMBER 3.0, Rev. A, University of California, San Francisco (1991); S. J. Weiner, P. A. Kollman, D. T. Nguyen, D. A. Case, *J. Comput. Chem.* **7**, 230 (1986).
37. Temperature was measured as described (*20*).
38. W. J. Becktel and J. A. Schellman, *Biopolymers* **26**, 1859 (1987).
39. S. Dao-pin, D. E. Anderson, W. A. Baase, F. W. Dahlquist, B. W. Matthews, *Biochemistry* **30**, 11521 (1991).
40. T. J. Richmond, *J. Mol. Biol.* **178**, 63 (1984).
41. F. M. Richards, *Annu. Rev. Biophys. Bioeng.* **6**, 151 (1977).

42. We are grateful for support by the Director, Office of Energy Research, Office of Basic Energy Sciences, Division of Material Sciences, and also by the Division of Energy Biosciences of the U.S. Department of Energy (DE-AC03-76SF00098). D.M. was supported by American Cancer Society postdoctoral fellowship PF-4014A and J.A.E. by NSF postdoctoral fellowship CHE-8907488. P.G.S. is an NSF Waterman Awardee. D.L.V. was supported by NIH through a Biotechnology Training Grant (GM-08388-02), and P.A.K. thanks NIH (GM-29072), for research support. We also thank the NIH for support of the UCSF Computer Graphics Laboratory, R. Langridge, P.I. (NIH-RR-1081).

26 February 1992; accepted 23 April 1992

Nuclear Localization of *Agrobacterium* VirE2 Protein in Plant Cells

Vitaly Citovsky, John Zupan, Debra Warnick, Patricia Zambryski*

The *Agrobacterium* single-stranded DNA (ssDNA) intermediate T-strand is likely transferred to the plant cell nucleus as a complex with a single VirD2 molecule at its 5′ end and multiple VirE2 molecules along its length. VirD2 contains a nuclear localization signal (NLS); however, because the T-strand is principally coated with VirE2 molecules, VirE2 also might assist in nuclear uptake. Indeed, VirE2 fused to a reporter protein localizes to plant cell nuclei, a process mediated by two amino acid sequences with homology to the bipartite NLS of *Xenopus* nucleoplasmin. Moreover, tumorigenicity of an avirulent *virE2* mutant is restored when inoculated on transgenic plants expressing VirE2, supporting in planta function of VirE2.

The interaction of *Agrobacterium* with plant cells results in crown gall tumors. Most functions for *Agrobacterium*–plant cell DNA transfer are carried on the Ti (tumor-inducing) bacterial plasmid. One portion, the T-DNA, is copied and transferred to the plant cell, but the products that mediate its movement are encoded by a separate virulence (*vir*) region. After induction of *vir* gene expression by small phenolic molecules excreted from wounded plant cells, a single-stranded copy of the T-DNA (T-strand) is generated and transferred [reviewed in (*1*)].

The T-strand associates with two protein products of the *vir* region, VirD2 and VirE2. The VirD2 protein is bound to the 5′ end of the T-strand (*2*), and an ssDNA binding protein (SSB), VirE2, coats the T-strand along its entire length (*3*, *4*). The T-strand associated with VirD2 and VirE2 is designated the T-complex (*5*). The T-complex travels from *Agrobacterium* into the plant cell where the T-DNA is integrated into the plant nuclear genome.

Recently, Howard *et al.* (*6*) identified a bipartite NLS at the COOH-terminus of VirD2; deletion of this sequence reduced *Agrobacterium* tumorigenicity (*7*). Thus, it was proposed that VirD2 mediates nuclear

V. Citovsky, J. Zupan, P. Zambryski, Department of Plant Biology, Genetics and Plant Biology Building, University of California, Berkeley, CA 94720.
D. Warnick, Sandoz Crop Protection Corporation, Palo Alto, CA 94304.

*To whom correspondence should be addressed.

uptake of the T-complex (6). However, the T-complex is a very large structure; a 20-kbp T-strand would contain about 600 molecules of VirE2 (4), have a combined molecular mass of about 50×10^6 daltons, and a predicted length of 3600 nm (5, 8, 9). Can such a large DNA-protein complex be transported into the nucleus by a single molecule of VirD2? Because VirE2 is a major protein component of the T-complex, it may assist in nuclear transport.

The coding sequence of the *virE2* locus was fused to the 3′ end of the β-glucuronidase (GUS) gene (Fig. 1A), and the resulting construct (10) was introduced into tobacco protoplasts. Intracellular localization of GUS-VirE2 was determined histochemically, with the GUS product of this fusion product localized specifically to the nucleus (Fig. 2C). GUS alone expressed in protoplasts did not exhibit nuclear localization (Fig. 2A). VirD2 expressed in tobacco protoplasts as a translational fusion with GUS also localized to the nucleus (Fig. 2B).

Many karyophilic proteins contain a bipartite NLS consisting of two basic regions separated by a variable number (but not less than 4) of spacer amino acids (11). Amino acid sequences of VirE2 proteins from nopaline (12) and octopine strains of *Agrobacterium* (13) reveal two regions with imperfect homology to the bipartite class of NLS exemplified by the NLS of *Xenopus* nucleoplasmin (Fig. 1B). Both these regions are homologous to the bipartite NLS of VirD2 (6) and are highly conserved in nopaline and octopine Ti plasmids. These putative NLS sequences were designated nuclear signal E1 (NSE 1), amino acid residues 228 to 244 and nuclear signal E2 (NSE 2), amino acid residues 296 to 310 (Fig. 1B).

To assay the role of NSE 1 and NSE 2 sequences in nuclear localization of VirE2, we constructed a series of single and double deletion mutants (del A to del E, Fig. 1A). Del A and del E lacked both NSE regions and were not localized to the nucleus. In contrast, del B mutant, which retains both NSEs, was localized to the cell nucleus. Deletion mutants that lacked only one NSE sequence (del C and del D) showed partial nuclear localization (Fig. 2 and Table 1).

To show that NSE 1 and NSE 2 are directly responsible for nuclear localization, three fusion proteins were constructed: GUS-NSE 1, GUS-NSE 2, and GUS-NSE 12 contain NSE 1, NSE 2, or both NSE 1 and NSE 2 signals in translational fusion to GUS (Fig. 1A). NSE 1 and NSE 2 were individually able to direct GUS to the nucleus with 68 and 78% efficiency, respectively (Table 1). Nuclear localization of the fusion protein containing both NSE sequences removed from the context of the native protein (GUS-NSE 12) was lower than that of the full-length VirE2 (Table 1), suggesting that the activity of the NSE signals depends on the surrounding protein context as previously observed for SV40 NLS and polyomavirus middle T antigen (14); it is possible that the two NSE signals may be augmented by the context of the native protein and may include other weak NLSs present elsewhere in VirE2.

We then studied the effect of deletion of the NSE sequences on VirE2 binding to ssDNA with mutants corresponding to del B, del C, del D, and del E (but not fused to GUS) (15). Full-length VirE2 binds ssDNA cooperatively (8): Even subsaturating amounts (5 to 10 μg) of VirE2 fully retarded the ssDNA probe (Fig. 3). Conversely,

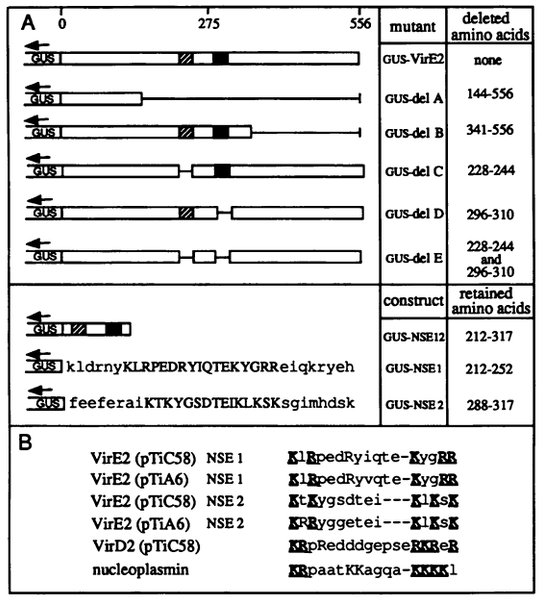

Fig. 1. Characterization of GUS-VirE2 deletion mutants and GUS-NSE constructs. (**A**) Physical maps. The numbers in the scale above refer to amino acids of VirE2 (wt) (12); thin lines indicate deleted regions; GUS indicates the GUS protein fused to VirE2 sequences; hatched and black boxes represent the NSE 1 and NSE 2 sequences, respectively. (**B**) Amino acid sequence homology between bipartite nuclear localization signals of *Agrobacterium* VirE2 [nopaline C58 (12) and octopine A6 strains (13)], VirD2 (6), and *Xenopus* nucleoplasmin (11). All basic residues are in upper case; basic amino acids of the two domains of bipartite signals are bold and underlined.

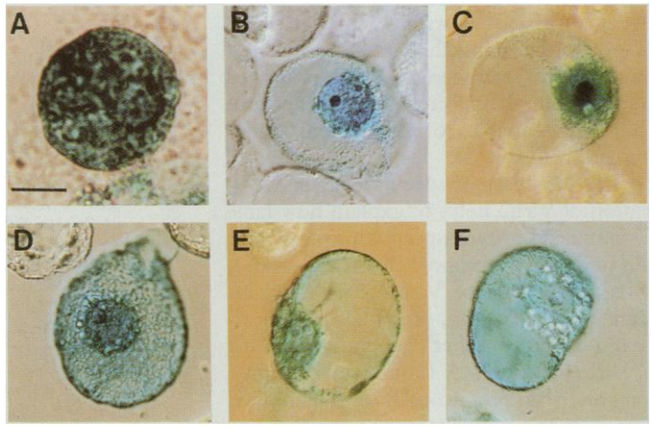

Fig. 2. Localization of GUS-VirE2 activity in tobacco protoplasts. *Nicotiana tabacum* (line XD) protoplasts were prepared, electroporated with supercoiled plasmids (50 μg), incubated in culture medium (18 to 20 hours), and assayed for GUS activity as described (6). (**A**) GUS alone; (**B**) GUS-VirD2; (**C**) GUS-VirE2; (**D**) GUS-del C; (**E**) GUS-del D; (**F**) GUS-del E. The length of the bar corresponds to 25 μm; all micrographs are at the same magnification.

Table 1. Quantification of nuclear and cytoplasmic levels of GUS activity. We quantified the intensity of indigo dye precipitates formed during the GUS assay in the plant cell cytoplasm and nucleus by photodensitometry, measuring the specific light transmission of the indigo GUS product in photographic negatives of single cells (6). Nuclear localization of GUS-VirE2 was defined as 100% activity, and GUS alone was defined as 0% activity. Each result is a mean value of independent measurements of ten different cells. Standard error values are in parentheses.

Construct	GUS activity (% of maximal)	
	Nucleus	Cytoplasm
GUS	0	100 (8)
GUS-VirE2	100 (5)	0
GUS-del A	8 (5)	92 (5)
GUS-del B	97 (2)	3 (2)
GUS-del C	76 (3)	24 (3)
GUS-del D	64 (2)	36 (2)
GUS-del E	0	100 (4)
GUS-NSE 1	68 (5)	32 (5)
GUS-NSE 2	78 (3)	22 (3)
GUS-NSE 12	82 (3)	18 (3)

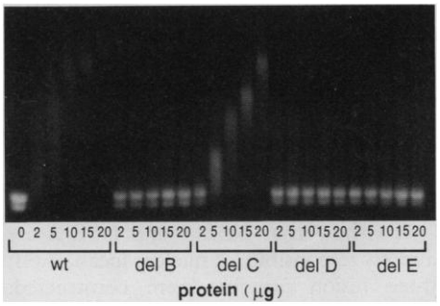

Fig. 3. ssDNA binding of VirE2 deletion mutants. The indicated amounts (micrograms) of purified VirE2 (wt) and its deletion mutants (del B to del E) were incubated for 10 min at 4°C in 40 μl of buffer L [10 mM tris-HCl (pH 8.0), 100 mM NaCl, 1 mM EDTA, and 10% glycerol] with 0.1 μg of M13 ssDNA (*8*). Incubation mixtures were separated by electrophoresis on a 3% agarose gel and stained with ethidium bromide (*17*).

del B was unable to bind ssDNA (Fig. 3), even though nuclear localization of del B was similar to that of the full-length VirE2 (Fig. 2C and Table 1). Thus, nuclear uptake of VirE2 does not require ability to bind ssDNA, and the two functions may be separable.

The separation between NLS and ssDNA binding activities, however, is not complete. Whereas the results with del B suggest that the ssDNA binding resides in the COOH-terminus of VirE2, the results with del D and del E indicate that other regions of the protein are also involved in this function. Del D and del E do not bind ssDNA (Fig. 3) and are also partly (del D) or completely (del E) unable to localize to the nucleus (Fig. 2 and Table 1). Inactivation of ssDNA binding in del D and del E may be due to conformational changes caused by these deletions. Changes in protein conformation after deletion of short stretches of amino acid residues were suggested to inactivate ss nucleic acid binding of the P30 protein of tobacco mosaic virus (*16*).

Del C is the only mutant in which both SSB and NLS functions are attenuated (Table 1 and Fig. 3). Binding of increasing amounts of del C results in mobility shifts proportional to the amount of protein added, which implies that the protein is randomly and equally distributed among all ssDNA molecules, characteristic of noncooperative binding (*17*).

The potential role of VirE2 in nuclear localization of the T-complex proposed here would imply an essential function of VirE2 inside the plant cell. To test this hypothesis, we produced transgenic tobacco plants that express the VirE2 protein (*18*). The ability of VirE2 transgenic plants to complement tumorigenicity of *virE2* mutants of *Agrobacterium* was tested (Table 2).

Table 2. VirE2 transgenic tobacco plants restore virulence of VirE2-deficient *Agrobacterium*. In two independent experiments, the top three nodes were removed from 6-cm-tall plants, and the cut surface was inoculated with pTiA6/pSM219 or pTiA6/pSM361 strains of *Agrobacterium* (10 μl of an overnight culture). Crown gall tumors were scored 2 weeks after inoculation. Data are expressed as number of plants that developed tumors per total number of infected plants. For VirE2 transgenic plants, three to four plants of each of the eight (VirE2), three (VirE3 del C), and four independent transformants (VirE2 del D) were inoculated.

Host, *Nicotiana tabacum*	Infecting *Agrobacterium*	
	pTiA6/pSM219	pTiA6/pSM361
Experiment 1:		
Wild type	4/4	0/5
Transgenic for VirE2	24/24	24/24
Transgenic for VirE2 del C	9/12	3/12
Transgenic for VirE2 del D	5/9	0/9
Transgenic for TMV P30	9/9	0/9
Experiment 2:		
Wild type	3/4	0/4
Transgenic for VirE2	17/27	23/29
Transgenic for VirE2 del C	7/11	2/11
Transgenic for VirE2 del D	6/10	0/11

Two *Agrobacterium* strains were used to infect plants: The pTiA6/pSM361 strain has an insertion mutation that inactivates the *virE* locus, and pTiA6/pSM219 has wild-type tumorigenicity on tobacco (*19*). Wild-type tobacco developed characteristic crown gall tumors when infected with pTiA6/pSM219 but not when inoculated with pTiA6/pSM361. Tumor formation by pTiA6/pSM361 was completely restored when inoculated on plants expressing VirE2. This complementation of tumorigenicity depended on the presence of both VirE2 NSE sequences. Complementation by transgenic plants expressing VirE2 del C or del D mutants was significantly reduced (del C) or completely blocked (del D) (Table 2). Although these results cannot separate overlapping NLS and SSB functions of VirE2, they strongly support the in planta function of this protein. Furthermore, plants transgenic for an unrelated SSB protein, P30 of tobacco mosaic virus (*20*), were unable to complement tumor formation (Table 2).

The discovery of specific nuclear localization of VirE2 helps to explain how large T-complexes are transported into the plant cell nucleus. We propose that the T-strand, with a molecule of VirD2 covalently attached to its 5′ end, is a folded and collapsed structure. After cooperative binding of VirE2, the ssDNA is unfolded to form a long and thin protein–ssDNA–T-complex. The T-strand is not sequence-specific; any DNA sequence located between the 25-bp T-DNA border repeats can be transported to plants (*1*). Thus, the T-strand apparently does not possess specific nucleotide sequences for nuclear uptake; instead, it likely is passively transported into the nucleus by its associated proteins [piggyback transport (*21*)]. This leaves only two components of the T-complex that might be responsible for nuclear transport—the VirD2 and VirE2 proteins—that each contain NLSs. Because full nuclear localization of VirE2 can only be achieved when two NLSs are present, the activity of each VirE2 NLS is intrinsically weaker than the single NLS of VirD2. We propose that the stronger NLS of VirD2 protein acts to initially target the T-complex to the nuclear pore in a polar fashion, facilitating uptake of the T-strand in a 5′ to 3′ direction. Polar transport of T-DNA has been proposed by earlier genetic and molecular studies of *Agrobacterium*-mediated plant cell transformation (*1*). VirE2 likely functions as a facilitator, making sure that the nuclear transport of the long and unfolded T-complex is not interrupted; furthermore, a large number of NLSs provided by VirE2 may increase the probability of T-complex interaction with the nuclear transport machinery (*22*).

There may be cellular proteins analogous to VirE2 that serve as molecular chaperones coating and unfolding nucleic acids and targeting them to and through nuclear pores. This idea suggests the intriguing possibility that nuclear transport of *Agrobacterium* T-complex may represent a generalized process of one of the mechanisms by which ssDNA or RNA molecules move within the cell, for example, as unfolded nucleic acid–protein complexes.

Note added in proof: In support of our model for nuclear uptake of thin, unfolded nucleic acid–protein complexes, Mehlin *et al.* (*22a*) describe translocation of the nuclear pore by a thin unfolded fiber of a premessenger ribonucleoprotein complex.

REFERENCES AND NOTES

1. P. Zambryski, *Annu. Rev. Plant Physiol. Plant Mol. Biol.* **43**, 465 (1992).
2. A. Herrera-Estrella, Z. Chen, M. Van Montagu, K. Wang, *EMBO J.* **7**, 4055 (1988); E. Ward and W. Barnes, *Science* **242**, 927 (1988); C. Young and E. W. Nester, *J. Bacteriol.* **170**, 3367 (1988); E. A. Howard, B. A. Winsor, G. De Vos, P. Zambryski, *Proc. Natl. Acad. Sci. U.S.A.* **86**, 4017 (1989).
3. C. Gietl, N. Z. Koukolikova, B. Hohn, *Proc. Natl. Acad. Sci. U.S.A.* **84**, 9006 (1987); P. J. Christie, J. E. Ward, S. C. Winans, E. W. Nester, *J. Bacteriol.* **170**, 2659 (1988); A. Das, *Proc. Natl. Acad. Sci. U.S.A.* **85**, 2909 (1988).
4. V. Citovsky, G. De Vos, P. Zambryski, *Science* **240**, 501 (1988).
5. E. A. Howard and V. Citovsky, *BioEssays* **12**, 103 (1990).
6. E. Howard, J. Zupan, V. Citovsky, P. Zambryski, *Cell* **68**, 109 (1992).
7. L. Hodges, C. Shurvinton, W. Ream, unpublished data.

8. V. Citovsky, M. L. Wong, P. Zambryski, *Proc. Natl. Acad. Sci. U.S.A.* **86**, 1193 (1989).
9. E. Howard, V. Citovsky, P. Zambryski, *UCLA (Univ. Calif. Los Angeles) Symp. Mol. Cell Biol. New Ser.* **129**, 1 (1990).
10. To monitor subcellular localization, we blunt-ended a VirE2 encoding sequence [1.7 kbp Nde I–Sal I fragment of pET3b:VirE2 plasmid (*4*)] into the Bgl II–Bam HI fragment of pRTL2SG-NIa/ΔB+K (*23*) (pGUS-E2). We constructed del A and del B by digestion of pGUS-E2 (Eco RI–Kpn I for del A and Sac I–Kpn I for del B), blunting the generated ends, and religation. Oligonucleotide-directed mutagenesis (*24*) of pGUS-E2 was used to construct the following deletion mutants: del C (residues 228 to 244), del D (residues 296 to 310), and del E (residues 228 to 244 and 296 to 310). We produced GUS-NSE 12 with the VirE2 295 bp Ssp I fragment as described for pGUS-E2. GUS-NSE 1 and GUS-NSE 2 were produced by oligonucleotide-directed mutagenesis of pGUS-NSE 12. We verified all deletions produced by oligonucleotide-directed mutagenesis by dideoxynucleotide sequencing (*25*).
11. J. Robbins, S. M. Dilworth, R. A. Laskey, C. Dingwall, *Cell* **64**, 615 (1991); C. Dingwall and R. A. Laskey, *Trends Biochem. Sci.* **16**, 478 (1991).
12. T. Hirooka, P. M. Rogowsky, C. I. Kado, *J. Bacteriol.* **169**, 1529 (1987).
13. S. C. Winans, P. Allenza, S. E. Stachel, K. E. McBride, E. W. Nester, *Nucleic Acids Res.* **15**, 825 (1987).
14. B. L. Roberts, W. D. Richardson, A. E. Smith, *Cell* **50**, 465 (1987).
15. To overproduce VirE2 and its derivatives, the Sal I restriction fragment of pET3b:VirE2 containing the VirE2 coding sequence under the T7 RNA polymerase promoter (*4*) was cloned into the Sal I site of pUC118 (p118E2). We produced del C, del D, and del E by oligonucleotide-directed mutagenesis of p118E2. We constructed del B by digesting pET3b:VirE2 with Sac I and religating. We produced VirE2, del B, del C, del D, and del E proteins in *Escherichia coli* strain BL21(DE3) with the T7 RNA polymerase expression system as described (*4, 8*).
16. V. Citovsky, M. L. Wong, A. Shaw, B. V. V. Prasad, P. Zambryski, *Plant Cell* **4**, 397 (1992).
17. T. M. Lohman, L. B. Overman, S. Datta, *J. Mol. Biol.* **187**, 603 (1986).
18. For production of VirE2 transgenic plants, a Cla I site was inserted directly upstream of the ATG translation initiation codon of the VirE2 coding sequence of p118E2 [or its del C and del D derivatives (*15*)] by oligonucleotide-directed mutagenesis, and the Cla I–Kpn I fragment of the resulting construct was cloned into pMON316 (*26*). To produce P30 transgenic plants, we used a polymerase chain reaction (*27*) to insert a Cla I site in front of the ATG translation initiation codon and a Kpn I site downstream of the amber stop codon of the P30-coding cDNA sequence of tobacco mosaic virus (*28*). The resulting modified fragment was cloned into the Cla I–Kpn I sites of pMON316. The recombinant pMON316 plasmids were transferred into *Agrobacterium* A208 strain carrying the disarmed pTiT37-SE plasmid (*26*) by electroporation (*Nicotiana tabacum* cv.). Turk leaf explants were infected with *Agrobacterium*, and the transgenic tobacco plants were regenerated as described (*29*). We verified transformants by assaying for neomycin phosphotransferase II (NPTII) (*30*), and we assayed the expression of VirE2 and P30 proteins by Western (protein) blot analysis of plant tissue extracts prepared as described (*31*).
19. S. E. Stachel and E. W. Nester, *EMBO J.* **5**, 1445 (1986).
20. V. Citovsky, D. Knorr, G. Schuster, P. Zambryski, *Cell* **60**, 637 (1990).
21. E. A. Nigg, P. A. Baeuerle, R. Luhrmann, *ibid.* **66**, 15 (1991).
22. L. Gerace and B. Burke, *Annu. Rev. Cell Biol.* **4**, 355 (1988).
22a. H. Mehlin, B. Daneholt, U. Skoglund, *Cell* **69**, 605 (1992).
23. J. C. Carrington, D. D. Freed, A. J. Leinicke, *Plant Cell* **3**, 953 (1991).
24. J. A. McClary, F. Witney, J. Geisselsoder, *BioTechniques* **7**, 282 (1989).
25. R. Kraft, J. Tardiff, K. S. Kranter, L. A. Leinwand, *ibid.* **6**, 544 (1988).
26. S. G. Rogers, H. J. Klee, R. B. Horsch, R. T. Fraley, *Methods Enzymol.* **153**, 253 (1987).
27. K. B. Mullis and F. Faloona, *ibid.* **155**, 335 (1987).
28. D. A. Knorr and W. O. Dawson, *Proc. Natl. Acad. Sci. U.S.A.* **85**, 170 (1988).
29. R. B. Horsch *et al.*, *Science* **227**, 1229 (1985).
30. R. E. McDonnel, R. D. Clark, W. A. Smith, M. A. Hinchee, *Plant Mol. Biol. Rep.* **5**, 380 (1987).
31. K. Lehto and W. O. Dawson, *Virology* **174**, 290 (1990).
32. We thank E. Howard and J. Carrington for discussions, S. Ruzin for advice on microscopy, and W. Ream for sharing results before publication. Supported by NSF (89-15613) and NIH (GM-45244-01) grants.

15 January 1992; accepted 27 April 1992

Overlapping But Nonidentical Binding Sites on CD2 for CD58 and a Second Ligand CD59

William C. Hahn, Elisabeth Menu, Alfred L. M. Bothwell, Peter J. Sims, Barbara E. Bierer*

The interaction of the T cell glycoprotein CD2 with one ligand, CD58, contributes to T cell function. We have identified CD59, a glycoprotein with complement-inhibitory function, as a second physiological ligand for CD2. Antibodies to CD59 inhibit CD2-dependent T cell activation in murine T cell hybridomas expressing human CD2. In an in vitro binding assay with purified CD58 and CD59, $CD2^+$ cells bind not only immobilized CD58 but also CD59. With two complementary approaches, it was demonstrated that the binding sites on CD2 for CD58 and CD59 are overlapping but nonidentical. These observations suggest that direct interactions between CD2 and both CD58 and CD59 contribute to T cell activation and adhesion.

Antigen-specific T cell immune responses depend on the expression of the T cell receptor (TCR)–CD3 complex; however, a number of other T cell–specific molecules play important roles in T cell activation and function (*1, 2*). Accessory molecules, such as CD2, function by facilitating adhesion, transducing signals that synergize with or modulate signals produced by the TCR-CD3 complex, or both. CD2 binds to lymphocyte function–associated antigen-3 (LFA-3, CD58), a broadly expressed 40- to 70-kD glycoprotein, and this receptor-ligand pair contributes both to T cell activation and to T cell adhesion with thymic epithelium, antigen-presenting cells, and erythrocytes (*1–3*). Although the interaction of CD2 with CD58 is important for T cell function, monoclonal antibody (MAb) inhibition studies have shown that at least one other erythrocyte protein, CD59, contributes to the phenomenon of spontaneous lymphocyte-erythrocyte rosetting, implying that a receptor for CD59 exists on the T cell (*4, 5*).

CD59 (protectin, HRF20, membrane inhibitor of reactive lysis) is a broadly distributed 18- to 20-kD membrane glycoprotein that restricts the lysis of human erythrocytes and leukocytes by human serum complement (*6–10*). To determine whether CD59 participates in T cell function by interacting with the CD2 molecule, we stimulated an antigen-specific murine T cell hybridoma that expresses the human CD2 molecule (*11*) with the human $CD58^+CD59^+$ Burkitt's lymphoma–derived B cell line Daudi. Expression of human CD2 in this hybridoma (16CD2-XH14) greatly enhanced the ability of these cells to respond to stimulation by Daudi as compared to the parent hybridoma (By155.16) (Fig. 1), and this enhancement was partially inhibited by either a purified, monospecific rabbit immunoglobulin G (IgG) to CD59 or an MAb to CD58 (Fig. 1). The simultaneous addition of antibodies to CD58 and CD59 resulted in complete inhibition of interleukin-2 (IL-2) production, suggesting that CD58 and CD59 each bind to CD2. In contrast, the addition of antibodies specific for either CD58 or CD59 did not inhibit the IL-2 response of a $CD2^-$ hybridoma that expresses the human CD4 molecule (16CD4-13) (*12*) (Fig. 1).

To assess whether $CD2^+$ cells bind CD59 directly, we tested the ability of

W. C. Hahn and E. Menu, Division of Pediatric Oncology, Dana-Farber Cancer Institute, and Harvard Medical School, Boston, MA 02115.
A. L. M. Bothwell, Section of Immunobiology, Yale Medical School, New Haven, CT 06510.
P. J. Sims, Cardiovascular Biology Research Program, Oklahoma Medical Research Foundation and Department of Microbiology and Immunology, Oklahoma University Health Sciences Center, Oklahoma City, OK 73104.
B. E. Bierer, Division of Pediatric Oncology, Dana-Farber Cancer Institute, and Harvard Medical School, and Hematology-Oncology Division, Department of Medicine, Brigham and Women's Hospital, and Department of Medicine, Harvard Medical School, Boston, MA 02115.
*To whom correspondence should be addressed.